Journal of Applied Physical Science International

Volume 16, Issue 1, Page 62-72, 2024; Article no.JAPSI.12186
ISSN: 2395-5260 (P), ISSN: 2395-5279 (O)

Magneto-optical Properties of Iron-bulk Metallic Glasses Sustainably Produced from Iron-rich Sand Sludge

Alfredo Antonio Alencar Exposito de Queiroz [a], Francisco de Assis Cavallaro [b] and Alvaro Antonio Alencar Queiroz [c*]

[a] Instituto de Física de São Carlos-Universidade de São Paulo (IFSC-USP), Av. Trabalhador São Carlense, 400 - Parque Arnold Schimidt, São Carlos - SP, CEP: 13566-590, Brazil.
[b] Universidade Cidade de São Paulo - UNICID, Rua Cesário Galeno, 448/475, São Paulo, São Paulo, CEP: 03071-000, Brazil.
[c] Instituto de Pesquisas Energéticas e Nucleares IPEN-CNEN, Centro de Biotecnologia, Av. Prof. Lineu Prestes, 2242, Cidade Universitária, São Paulo – SP, 05508-000, Brazil.

Authors' contributions

This work was carried out in collaboration among all authors. Author AAAEdeQ managed the Raman analyses, and literature searches. Author FdeAC designed the study, and wrote the protocol. Author AAAQ managed the analyses of the study, and wrote the first draft of the manuscript. All authors read and approved the final manuscript.

Article Information

DOI: https://doi.org/10.56557/japsi/2024/v16i18742

Open Peer Review History:
This journal follows the Advanced Open Peer Review policy. Identity of the Reviewers, Editor(s) and additional Reviewers, peer review comments, different versions of the manuscript, comments of the editors, etc are available here: https://prh.ikprress.org/review-history/12186

Original Research Article

Received: 16/04/2024
Accepted: 18/06/2024
Published: 25/06/2024

ABSTRACT

A large amount of sand sludge (SS) from rivers polluted with heavy metals is continuously dredged and often dumped into landfills, resulting in environmental pollution of soil and water. This work examines the feasibility of the utilization of iron-enriched SS from dredged polluted rivers to produce Fe-based bulk metallic glasses (Fe-BMG). Fe-BMG was prepared from SS by melt-quenching

**Corresponding author: E-mail: alvaro.queiroz@ipen.br;*

Cite as: *Queiroz, Alfredo Antonio Alencar Exposito de, Francisco de Assis Cavallaro, and Alvaro Antonio Alencar Queiroz. 2024. "Magneto-Optical Properties of Iron-Bulk Metallic Glasses Sustainably Produced from Iron-Rich Sand Sludge". Journal of Applied Physical Science International 16 (1):62-72. https://doi.org/10.56557/japsi/2024/v16i18742.*

technique, and their magnetic and photochromic properties were studied. The chemical composition of the Fe-BMG was determined by X-ray fluorescence (XRF). The structural properties have been analyzed using the Raman spectroscopy (RS), vibrating sample magnetometer (VSM) and ultraviolet-visible (UV-VIS) spectroscopy. XRF results shows that Fe-BMG contains an iron proportion of 38.8% (wt.) as the hematite (α-Fe_2O_3), and magnetite (Fe_3O_4) phases. The Raman "fingerprints" of α-Fe_2O_3 and Fe_3O_4 were identified at 1330 cm^{-1}, and 300-600 cm^{-1}, respectively. The measured saturation magnetization of Fe-BMG samples is 3.0 emu/g at 60 kOe. A UV-VIS analysis of the Fe-BMG exposed to sunlight simulator reveals an enhanced transmission of light in the 400-700 cm^{-1} region. These findings confirmed the successful conversion of the hazardous SS into Fe-BMG with promising magneto-optical characteristics for a wide variety of technological applications.

Keywords: Urban sand sludge; magnetic glass; x-ray fluorescence analysis; iron-rich glasses; Raman spectroscopy; hematite.

1. INTRODUCTION

Pinheiros River (PR) is one of the most important rivers in Southeast Brazil (SE) and crosses the metropolitan region of São Paulo city, the largest metropolis of Latin America and the main industrial center in the country (Fig. 1a) [1]. The PR is an affluent 25 km long affluent of the Tietê River and rises from the meeting of the Guarapiranga River with the Rio Grande. In the past, these three rivers formed a single one, with springs located in Serra do Mar and mouths in Tietê River. The PR network is very important for the economy of the southeast region due to its high electrical potential producing more than 1 GW of electricity and mainly due to its high potential for the construction of urban waterways [2].

The history of PR is closely related to the human activities developed in its surroundings which contributed to its degradation due to the irregular dumping of industrial and urban waste from the metropolitan region of São Paulo city in the riverbed (Fig. 1b) [3-5]. This practice became common due to the absence of a sewage collection network in the period of Brazilian industrialization during the period from 1930 to 1970 [6].

Annually, about 2.10^5 m^3 of sediments are deposited in the PR at the stretch that crosses the metropolitan region of São Paulo city [7]. As consequence of this deposition process, there is an intense silting of the river, forming sandbanks that alter the flow and volume of water that impair its navigability [8]. In addition, the width of the river increases and the water temperature also rises by losing depth due to the accumulation of sediments and the greater irradiation of the sun per area, respectively. The presence of sediments also darkens the river water preventing the penetration of light making PR biologically dead and extremely harmful to human health within the metropolitan region of São Paulo city, which stretches for about one hundred kilometers [9,10].

Nowadays, the PR basin is already undergoing a process of desanding and dredging (Fig. 1c) with the removal of approximately three million of cubic meters per year of sediment and garbage [4]. The composition of the sediment extracted in the desanding process is approximately 64.46% of sand, making the reuse of this material very attractive due to the high volume of material dredged annually [4]. As there are no suitable places for the disposal of waste, this results from the de-silting of the PR within the metropolitan region of São Paulo city. The solution found for the high volume of sediments removed annually is to send them to landfills, competing with urban and residential waste at very high costs. Therefore, the reuse of the sand from PR will play an essential role in saving inputs and the reduction of environmental pollution in the metropolitan region of São Paulo city.

The physical-chemical studies of the PR sand sludge (SS) revealed that the contamination is mainly composed of heavy metals, especially iron oxides [11-13]. The main sources of metal emissions are the megacity of São Paulo (11 million people and many metal processing workshops), improper battery disposal, real estate developments, and its metallurgic industries [14]. Solutions that prioritize technology and the environment are essential for the use of PR sediments, thus investing in technology and reducing the unbridled consumption of the planet's natural resources.

Fig. 1. Location of the Pinheiros river in the urban area of the São Paulo-Brazil (a,b), accumulation of sand banks (c) and desilting as part of the sand sludge removal process (d)

The production of new materials from PR SS in a sustainable way seems interesting and requires a mastery of techniques and optimization of inputs, energy matrices, and the waste use always aiming at the quality of the environment. Among the alternatives for using the SS from the PR, its use as a raw material for the manufacture of magnetic glass stands out, because it contains a high content of silica and iron in its composition.

Despite the large number of investigations about waste and industrial residues as raw material for the production of functional glasses and glass ceramics [15] there are incipient studies on the use of SS dragged from polluted rivers in Brazil [16] and, as far as the authors are aware, no investigations regarding its use in the preparation of magneto-optical glasses were reported till the moment.

This work explores the potential applications of SS from PR for the production of iron-bulk metallic glasses (Fe-BMG) with interesting magneto-optical properties for engineering applications. Fe-BMG have attracted interest because of their excellent engineering properties such as thermal resistance, corrosion resistance, mechanical strength [17] and excellent magnetic properties that would be interesting for use in power engineering [18] and medicine [19].

2. MATERIALS AND METHODS

2.1 Sampling and Fe-BMG Glasses Production

The bottom sediment of SS samples was collected in the PR at the site in -23°3'21.59" to South latitude and meridians -46°44'59.99" West longitude, region of the metropolitan region of São Paulo city. To obtain a representative sample from each sampling site, samples of SS dredged from the PR were collected at five different points, separated by approximately 2 m. All sampling was carried out with plastic shovels to avoid contamination of the samples. Material from individual sites was mixed into a sample with a total mass of about 1.0 kg, representative of the respective site. The solid residue of SS was dried in the open air until the mass was constant followed by manual crushing.

The raw materials used in the production of the Fe-BMG are indicated in Table 1. A total mass of 1.0 kg of the raw materials was mixed in a shaker mixer. The melting was carried out in a melting furnace based on biogas (Sabesp-SP) with a heating rate of 10ºC/min up to 1550 ºC and maintained for one hour at the established level.

Table 1. General proportions by weight of the raw materials for the Fe-BMG production

Component	Proportion by weight (wt.%)
Na_2O	15.0
CaO	10.0
Al_2O_3	1.0
SiO_2 (Sand Sludge)	64.46
Iron Oxides (in Fe_2O_3)	38.80

The biogas-based furnace promotes lower emission of greenhouse gases, and energy savings during the Fe-BMG manufacturing process. The Pt crucible and contents were then removed from the furnace and the molten glass was poured into cold water to avoid crystallization.

2.2 Structural and Physical Properties of Fe-BMG

The density of the iron-bulk metallic glasses has been measured at room temperature (25 °C) using the Archimedes method using water as immersive fluid. The iron-bulk metallic glasses sample was immersed in water and its density was calculated by Equation (1) [20]:

$$\rho_G = \frac{m_G}{[m_G + (m_W - m_{W+G})]} \cdot \rho_W \qquad (1)$$

where ρ_G is the glass density, m_G is the weight of glass measured in air, m_W is the weight of water only, m_{W+G} is the weight of glass immersed in water and ρ_W is the water density (0.9970 g/cm^3 at 25 °C).

Compositions of the SS and Fe-BMG samples were obtained by the energy dispersive X-ray fluorescence (XRF) (XRF Shimadzu, EDX-720/800HS spectrometer) using a rhodium (Rh) source for the excitations. The scans were performed over the energy range of the sodium (Na) to Uranium (U) oxides at room temperature (25 °C) and atmospheric pressure conditions. A polypropylene sample holder was used. An area of approximately 100 mm^2 of the iron-bulk metallic glass sample was analyzed.

The Raman spectrum for the identification of the iron oxide phase present in Fe-BMG was measured in a LabRAM HR Evolution Raman spectrometer (Horiba Scientific) equipped with a Czerny-Turner monochromator, a CCD detector, and an Olympus confocal microscope (50X objectives). The laser excitation of a line at 532 nm was employed with a power of 3.875 mW on the surface of the samples. A diffraction grating with a density of 600 lines.mm^{-1} and a resolution of 2 cm^{-1} was used.

The magnetic characteristic of the Fe-BMG was analyzed using a vibrating sample magnetometer model EZ9, MicroSense. The applied magnetic field was varied between 20 and -20 kOe and measured at room temperature (25 °C).

Polished Fe-BMG plates with 200 mm^2 dimensions and about 2 mm thickness were irradiated, using a xenon arc lamp (Xe) simulating the full spectrum of sunlight. The absorbance of samples was collected before then and after 90 min of irradiation time, using a double beam spectrophotometer (Shimadzu, UV-VIS-NIR, UV-3600 i) with wavelengths ranging from 185 to 3300 nm and spectral bandwidth of 0.1 nm.

3. RESULTS AND DISCUSSION

3.1 Fe-BMG Composition and Density

Fig. 2 shows the elemental compositions of the Fe-BMG samples analyzed using quantitative XRF. Results of the XRF analysis shows the following elements (expressed as oxides in mol percentages): SiO_2 (64.46%), Al_2O_3 (1.29%), Fe_2O_3 (38.80 %), Cr_2O_3 (1.61 %), NiO (1.24%), Mn_2O_3 (1.43%), CuO (0.25%). Iron (Fe) is the most dominant magnetic element, along with a small composition of other transition elements that also have interesting optical and magnetic properties, such as Cr, Ni, and Mn, which are in oxide forms. Considering the higher content of iron, the d-orbitals of this element are not shielded by outer orbitals so that the Laporte selection rules suffer relaxation, resulting in the intense brownish-black coloration of Fe-BMG (Fig. 3(a)) [21]. The observed black color is indicative of Fe_3O_4, and the brown color can be strongly related to the d-d transitions in (α-Fe_2O_3) (Fig. 3(a)).

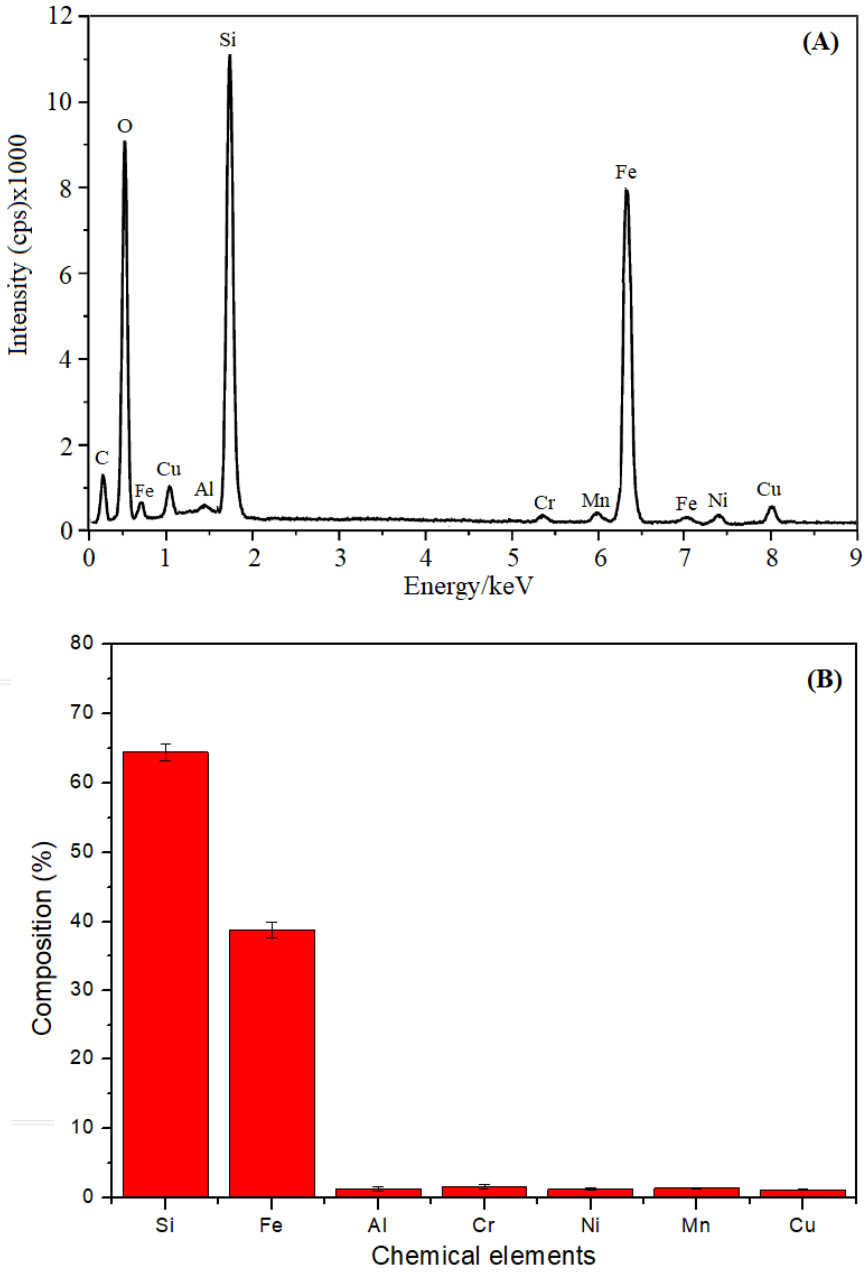

Fig. 2. X-ray fluorescence spectra of the Fe-BMG (a) and its chemical composition (b)

It is well known that pure SiO_2 glass is essentially composed of a continuous random network of corner-sharing SiO_4 tetrahedra where each oxygen atom bridges two tetrahedrons [22]. The presence of α-Fe_2O_3, maghemite (γ-Fe_2O_3) and magnetite (Fe_3O_4) causes the breaking of the glass network where each Si atom remains four-fold coordinated to oxygen but some of these oxygen atoms are non-bridging resulting in a network of iron oxides and SiO_2 molecules. The density and molar volume values for Fe-BMG were 4.4865 $g.cm^{-3}$ and 26.9166 $mol.cm^{-3}$, respectively. These values are significantly higher than that value observed for alkali borophosphate glasses, and suggest that the presence of Fe_2O_3 causes shrinkage of the glass network which increases density [23].

3.2 Structural Characterization of Fe-BMG by Raman Spectroscopy

The Raman spectrum of Fe-BMG is shown in Fig. 3(b). The main feature of the Raman spectra of Fe-BMG are the broad bands

observed at the low-wavenumber region (250-650 cm^{-1}), the mid-wavenumber region (650-850 cm^{-1}), and in the high-wavenumber region (850-1700 cm^{-1}). The low-wavenumber region was assigned to vibrations of Si-O bonds in silicate networks and Fe-O bonds in maghemite (γ-Fe_2O_3), α-Fe_2O_3, and Fe_3O_4 structures [24,25]. The mid-wavenumber region band appears to be related to the symmetric stretching vibrations mode of SiO_4 tetrahedrons resulting from differences in the organization of the Fe-BMG structure [26]. The band with very low intensity observed at 690 cm^{-1} is characteristic of residual ferrihydrite ($Fe(OH)_3$) [27]. The well-established α-Fe_2O_3 bands are visible at 1330 cm^{-1}, and additional bands are observed at 1440 cm^{-1}, and 1550 cm^{-1}, which is similar to the spectrum reported for γ-Fe_2O_3 [28].

The Raman spectra (Fig. 3(b)) suggests that SS from PR appears to contain a large amount of iron oxides and oxyhydroxides, being largely amorphous oxyhydroxides, known as $Fe(OH)_3$, which could be retained as solid phases in the SS of PR [29,30]. The high temperature used in the Fe-BMG glasses manufacturing process causes Fe $(OH)_3$ dehydration, forming γ-Fe_2O_3 and α-Fe_2O_3, which are more thermodynamically stable. Fig. 4 illustrates the mechanism of the coexistence of the α-Fe_2O_3 and γ-Fe_2O_3 on the Fe_3O_4 surface after Fe-BMG manufacturing.

The ferrihydrite precipitated in SS of PR forms a redox couple with the sulfide and the ferrous ion (Fe^{2+}), which is the resulting of the high electron current density needed for the solid-state transformation of ferrihydrite ($Fe(OH)_3$) to thermodynamically more stable Fe_3O_4 phase. The heating of SS from PR at 1550 ^oC in hydrothermal conditions for Fe-BMG processes, results in the formation of the maghemite (γ-Fe_2O_3), and hematite (α-Fe_2O_3) phases directly on the magnetite (Fe_3O_4) surface. Fig. 5 illustrates the chemical cycling of iron in water of the polluted PR regulated by electron transfer processes mediated by anaerobic microorganisms.

3.3 Magnetic and Optical Properties of Fe-BMG

The magnetic hysteresis curve measured at room temperature (25^oC) of the Fe-BMG samples is shown in Fig. 6. The samples show a saturation magnetization of about 3.0 $emu.g^{-1}$ at 60 kOe, which suggests a ferromagnetic behavior of magnetite and hematite. This result is in agreement with other studies previously published on soft ferromagnetic bulk metallic glasses [31].

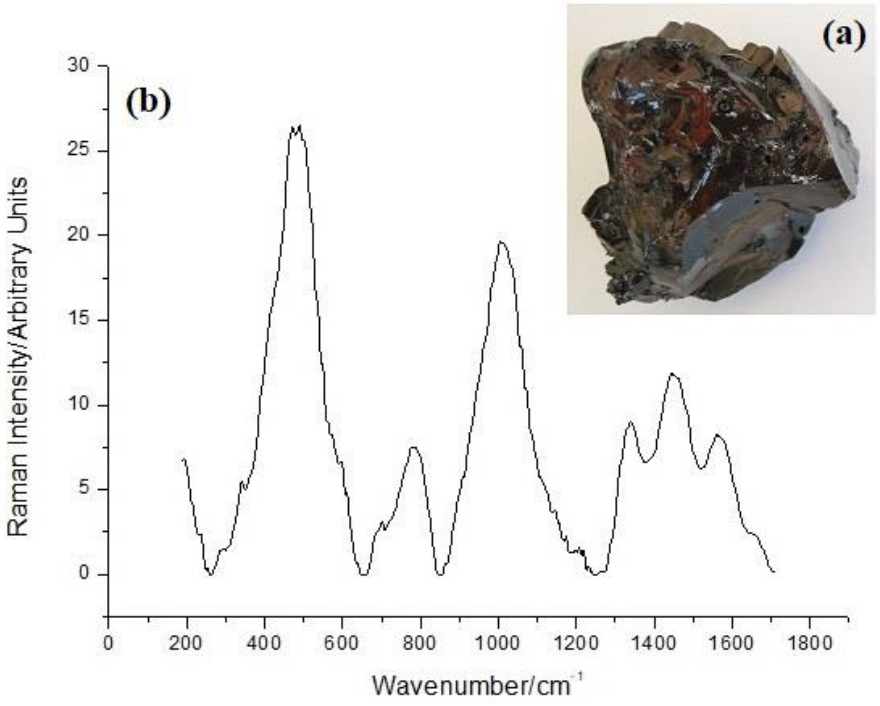

Fig. 3. Sample of the Fe-BMG glass produced (a), and its Raman spectrum (b)

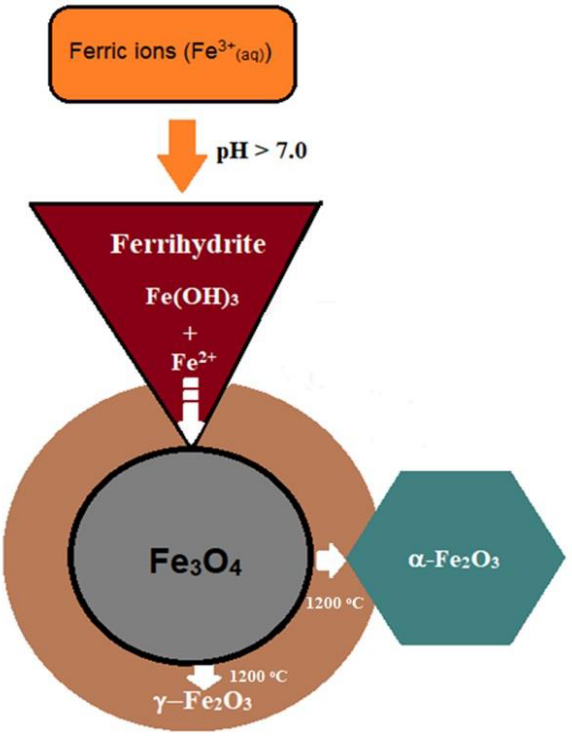

Fig. 4. Possible mechanisms of the formation of magnetite (Fe_3O_4), maghemite (γ-Fe_2O_3), and hematite (α-Fe_2O_3) phases during the Fe-BMG manufacturing process

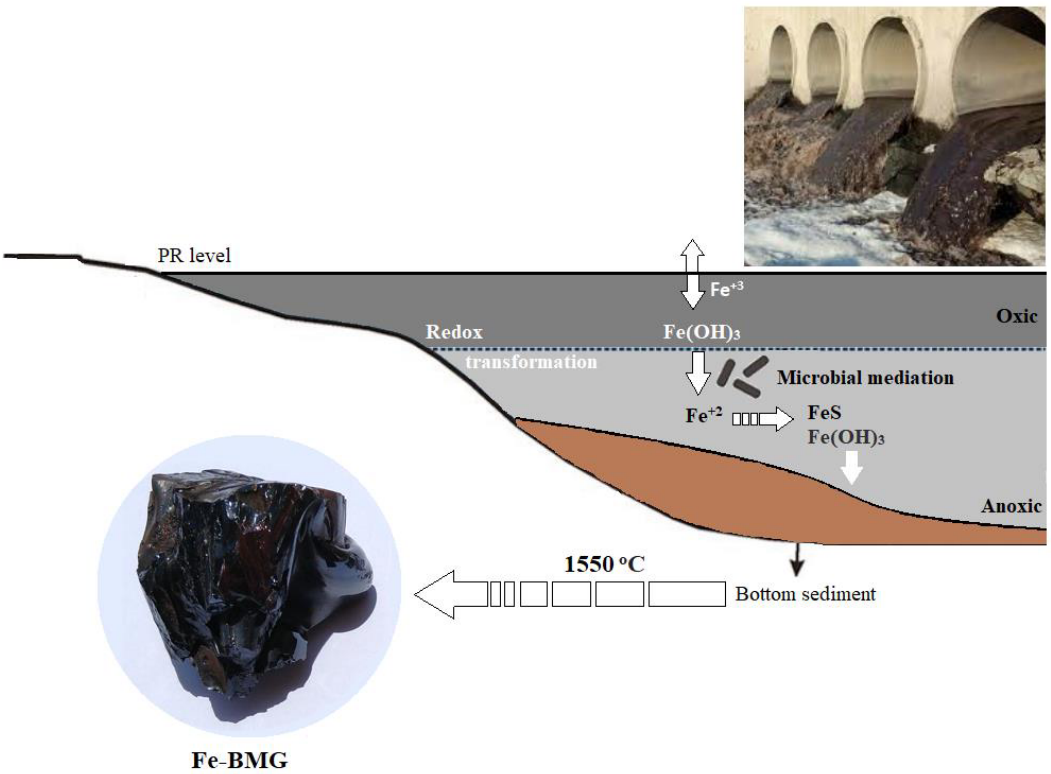

Fig. 5. Precipitation pathways for ferrihydrite, and iron sulfide formation that are deposited on the river bottom with the sand sludge

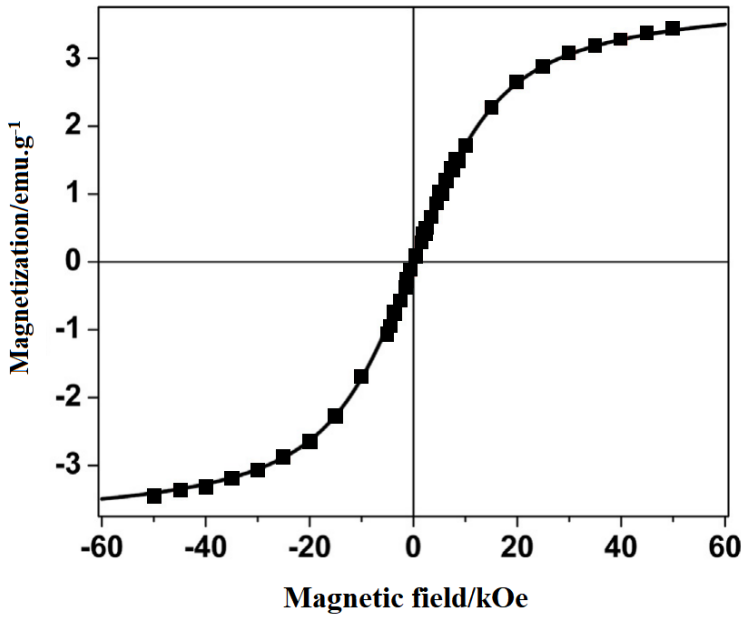

Fig. 6. Magnetization curve of the Fe-BMG sample measured at room temperature (25 °C).

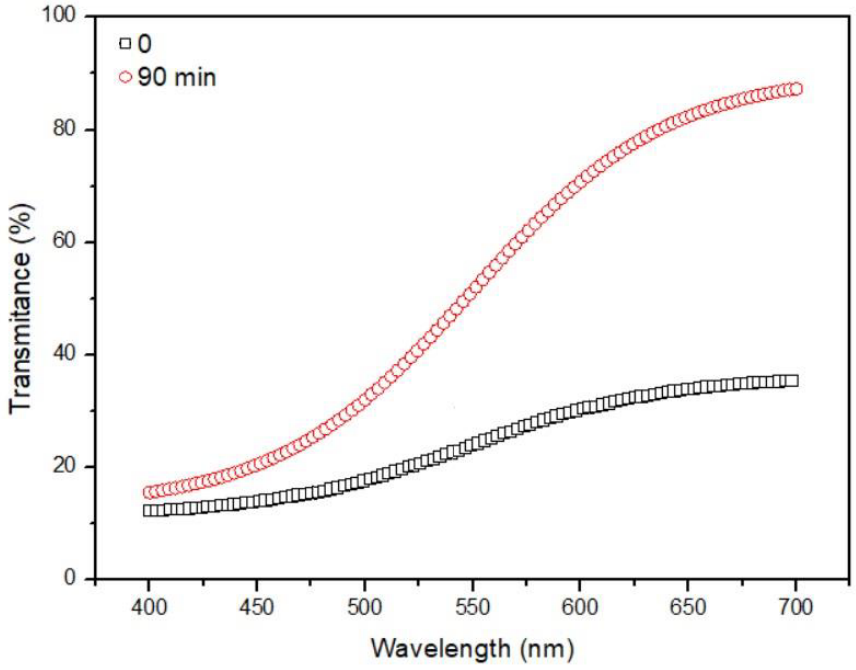

Fig. 7. Spectral transmittance of Fe-BMG before (□) and after (○) irradiation with UV Xe arc lamp for 90 min at room temperature (25 °C)

Fig. 7 depicts the UV-VIS transmission spectra of Fe-BMG plates unexposed and exposed to sunlight simulator (Xe arc lamp). The strong and enhanced absorption of Fe-BMG in the visible region can be attributed to the creation of defects-type non-bridging oxygen hole centers (NBOHCs) at the glass matrix. NBOHCs have strong absorption in the visible region of the electromagnetic spectrum, which gives glasses a reddish-brown color in soda-lime glasses containing iron oxides. The electrons released by the NBOHCs defects are trapped by Fe^{3+}, thus favoring the indirect charge transition 3d→3d of Fe^{3+} contributing to a high transmission in the visible region of the electromagnetic spectrum (Fig. 7) [32].

4. CONCLUSIONS

In this work, Fe-BMG with iron oxides content of 38.8% was successfully prepared by a melt-quenching method from sand sludge dredged from polluted river. The structural, optical, and magnetic properties of Fe-BMG samples were studied. The density, and molar volume of Fe-BMG were 4.4865 $g.cm^{-3}$, and 26.9166 $mol.cm^{-3}$, respectively, suggesting that the presence of iron oxides causes the opened glass network structure. The Raman spectra and magnetic results could confirm the presence of α-Fe_2O_3, and Fe_3O_4 in the Fe-BMG structure. After exposure to artificial sunlight, the transmittance of the Fe-BMG samples increases considerably after 90 min of irradiation time in the visible region (450-700 nm) due to the charge transition 3d→3d of Fe^{3+}.

DISCLAIMER (ARTIFICIAL INTELLIGENCE)

Author(s) hereby declare that no generative AI technologies such as Large Language Models (ChatGPT, COPILOT, etc) and text-to-image generators have been used during writing or editing this manuscript.

ACKNOWLEDGEMENTS

This research was partially funded by the National Council for Scientific and Technological Development (CNPq).

COMPETING INTERESTS

Authors have declared that no competing interests exist.

REFERENCES

1. Da Luz RA, Rodrigues C. The historical process of occupation and floods on the Pinheiros River´s fluvial plain from 1930 to the present days. Geousp. 2020;24:340-360.
Available:https://doi.org/10.11606/issn.2179-0892.geousp.2020.164499
2. Hochstetler RL, Cho JD. Assessing competition in Brazil's electricity market if bid-based dispatch were adopted. Revista de Economia Contemporânea. 2019;23:1-37.
Available:https://doi.org/10.1590/198055272322
3. Battibugli, Agencia Brasil A. Government of São Paulo announces 530,000 sewage connections on the Pinheiros River. See São Paulo; 2020.
Available:https://vejasp.abril.com.br/cidades/esgoto-rio-pinheiros/
4. Uol news; 2024.
Available:https://f.i.uol.com.br/folha/publicidade/images/14196691.jpeg
5. DAEE Renews contract to desilt 41 km of the Tietê River; 2021.
Available:https://www.apelmat.org.br/daee-renova-contrato-para-desassorear-41-km-do-rio-tiete/
6. Cunha DGF, Grull D, Damato M, Blum JRC, Eiger S, Lutti JEI, Mancuso PCS. Contiguous urban rivers should not be necessarily submitted to the same management plan: The case of Tiete and Pinheiros River (Sao Paulo-Brazil). Annals of the Brazilian Academy of Sciences. 2011;83:1465-1480.
Available:https://doi.org/10.1590/S0001-37652011000400032
7. Costa SB, De Almeida Filho GS, Giudice SL, Hellmeister Z Jr. Panorama of desilting in the Tietê and Pinheiros rivers, São Paulo, Brazil. XX Brazilian Symposium on Water Resources, 17-22 November Bento Gonçalves/RS; 2013.
Available:https://files.abrhidro.org.br/Eventos/Trabalhos/66/SBRH2013__PAP012905.pdf
8. Smith WS, Da Silva FL, Biagioni RC. River dredging: When the public power ignores the causes, biodiversity and science. Environment and Society. 2019;22:1-20.
Available:https://doi.org/10.1590/1809-4422asoc0057r1vu19L1AO
9. Abraham WR. Megacities as sources for pathogenic bacteria in rivers and their downstream fate. International Journal of Microbiology. 2011;2011:798292.
Available:https://doi.org/10.1155/2011/798292
10. Godoy RG, Marcondes MA, Pessôa R, Nascimento A, Victor JR, Duarte da Silva AJ, Clissa PB, Sanabani SS. Bacterial community composition and potential pathogens along the Pinheiros River in the southeast of Brazil. Scientific Reports. 2020;10:9331.
Available:https://doi.org/10.1038/s41598-020-66386-y
11. Da Silva IS, Abate G, Lichtig J, Masini JC. Heavy metal distribution in recent

sediments of the Tietê-Pinheiros river system in São Paulo state, Brazil. Applied Geochemistry. 2002;17:105-116.
Available:https://doi.org/10.1016/S0883-2927(01)00086-5

12. Mortatti J, Probst JL, De Moraes GM. Heavy metal distribution in recent sediments along the Tietê River basin (São Paulo, Brazil). Geochemistry Journal. 2012;46:13-19.
Available:https://doi.org/10.2343/geochemj.1.0136
13. Rocha FR, Silva PSC, Castro LM, Bordon ICCL, Oliveira SMB, Favaro DIT. NAA and XRF technique bottom sediment assessment for major and trace elements: Tietê River, São Paulo State, Brazil. Journal of Radioanalytical and Nuclear Chemistry. 2015;306:655-665.
Available:https://doi.org/10.1007/s10967-015-4261-8.
14. Favaro DIT, Rocha FR, Angelini M, Henriques HRA, Soares JS, Silva PSC, Oliveira SMB. Metal and trace element assessments of bottom sediments from medium Tietê River basin, Sao Paulo State, Brazil: Part II. Journal of Radioanalytical and Nuclear Chemistry. 2018;316:805-818.
Available:https://doi.org/10.1007/s10967-018-5821-5
15. Chinnam RK, Francis AA, Will J, Bernardo E, Boccaccini AR. Review-Functional glasses and glass-ceramics derived from iron rich waste and combination of industrial residues. Journal of Non-Crystalline Solids. 2013;365:63-74.
Available:https://doi.org/10.1016/j.jnoncrysol.2012.12.006
16. Heinrich AB, Metzger JW, Fischer KM, Mathias AL. Sediment management from dredging of an urban river: Case study of the lower Belem river. Brazilian Journal of Soil Science. 2015;39:626-636.
Available:https://doi.org/10.1590/01000683rbcs20140091
17. Gao K, Zhu XG, Chen L, Li WH, Xu X, Pan BT, Li WR, Zhou WH, Li L, Wang W, Li Y. Recent development in the application of bulk metallic glasses. Journal of Materials Science and Technology. 2022;131:115-221.
Available:https://doi.org/10.1016/j.jmst.2022.05.028
18. Khan MM, Nemati A, Rahman Z, Shah UH, Asgar H, Haider W. Recent advances in bulk metallic glasses and their applications: A review. Critical Reviews in Solid State and Materials Science. 2018; 43:233-268.
Available:https://doi.org/10.1080/10408436.2017.1358149
19. Li HF, Zheng YF. Recent advances in bulk metallic glasses for biomedical applications. Acta Biomaterialia. 2016;36: 1-20.
Available:https://doi.org/10.1016/j.actbio.2016.03.047
20. ASTM C373. Standard test method for water absorption, bulk density, apparent porosity and apparent specific gravity of fired whiteware products, ASTM Int., West Conshohocken; 1988.
21. Laporte O, Meggers WF. Some rules of spectral structure. Journal of the Optical Society of America. 1925;11:459-463.
Available:https://doi.org/10.1364/JOSA.11.000459
22. Onodera Y, Kohara S, Salmon PSAH,. Structure and properties of densified silica glass: Characterizing the order within disorderer. NPG Asia Materials. 2020;12:1-16.
Available:https://doi.org/10.1038/s41427-020-00262-z
23. Chi Y, Lin J, Xu B. Effects of Fe2O3 on the properties of glass foams prepared by iron-containing solid waste. Glass Physics and Chemistry. 2019;45:104-110.
Available:https://doi.org/10.1134/S1087659619020056
24. Hanesch M. Raman spectroscopy of iron oxides and (oxy) hydroxides at low laser power and possible applications in environmental magnetic studies. Geophysical Journal International. 2009; 177:941-948.
Available:https://doi: 10.1111/j.1365-246X.2009.04122.x
25. Chernyshova IV, Hochella MF, Maddenc AS. Size- dependent structural transformations of hematite nanoparticles. 1. Phase transition, Physical Chemistry Chemical Physics. 2007;9:1736-1750.
Available:https://doi.org/10.1039/b618790k
26. Liu H, Hahn SH, Ren M, Thiruvillamali M, Gross TM, Du J, Van Duin ACT, Kim SH. Searching for correlations between vibrational spectral features and structural parameters of silicate glass network. Journal of the American Ceramic Society. 2020;103:3575-3589.
Available:https://doi.org/10.1111/jace.17036.

27. Cudennec Y, Lecerf A. The transformation of ferrihydrite into goethite or hematite, revisited. Journal of Solid State Chemistry. 2006;179:716-722. Available:https://doi.org/10.1016/j.jssc.2005.11.030
28. Mazzetti L, Thistlethwaite PJ. Raman spectra and thermal transformations of ferrihydrite and schwertmannite. Journal of Raman Spectroscopy. 2002;33:104-111. Available:https://doi.org/10.1002/jrs.830
29. Silva I, Abate G, Lichtig J, Masini J. Heavy metal distribution in recent sediments of the Tietê-Pinheiros river system in São Paulo state, Brazil. Applied Geochemistry. 2002;17:105-116. Available:https://doi.org/10.1016/S0883-2927(01)00086-5
30. Ustra AT, Mendonça C, Da Silva Leite A, Macouin M, Doherty R, Respaud M, Tocuti G. Ultrafine magnetic particles: A DIET-proxy in organic rich sediments? Frontiers in Earth Science. 2021;8:1-11. Available:https://doi.org/10.3389/feart.2020.608387
31. Ramasamy P, Stoica M, Ababei G, Lupu N, Eckert J. Soft ferromagnetic bulk metallic glass with potential self-healing ability. Materials. 2020; 13:1-8. Available:https://doi.org/10.3390/ma13061319
32. Zhang Z, Hossain F, Takahas T. Fabrication of shape-controlled α-Fe_2O_3 nanostructures by sonoelectrochemical anodization for visible light photocatalytic application. Materials Letters. 2010;64:435-438. Available:https://doi.org/10.1016/j.matlet.2009.10.071

Peer-review history:
The peer review history for this paper can be accessed here:
https://prh.ikprress.org/review-history/12186